Numerical computation of electromagnetically sourced nonlinear tails

Zhen-Tao He

University of Chinese Academy of Sciences

Oct. 18, 2025
@the Two Mountains High-Level Talents Area

Based on arXiv: 2508.20499
with Jia Du, Jiageng Jiao, Caiying Shao, Junxi Shi, Yu Tian, and Hongbao Zhang.

Current Section

Nonlinearities in black hole (BH) ringdown

- Recently, increasing studies reveal rich phenomena arising from nonlinearities in BH ringdown, such as quadratic QNMs and nonlinear power-law tails [see a recent review 2505.23895].
- Not only can the quadratic QNM's amplitude be even larger than that of their linear counterpart [Mitman et al., PRL(2023); Cheung et al., PRL(2023)],
- but the nonlinear tails can decay more slowly than the linear Price's law. [Cardoso et al., PRD(2024); Marina et al., 2412.06887; Ma et al., PRD(2025); Kehagias et al., PRD(2025); Ling et al., PRD(2025)]

Motivation

- Transient electromagnetic events in the astrophysical environment are typically high-energetic, potentially responsible for some nonlinearities in ringdown.
- If a neutron star has magnetic energy up to 10^{49} ergs and a mass of about one solar mass $M_\odot$, then its EM effect could surpass its second-order gravitational effect in extreme mass ratio inspiral systems with a supermassive BH $M \gtrsim 10^6 M_\odot$.
- Hence, the multi-messenger astronomy, which integrates GW detection and EM observation, could help the interpretation of GW signals.
- For example, by analysing the QNMs of GWs generated from transient high-energetic EM waves, one can detect solitary black holes, whose number and distribution in the Milky Way encode essential information about BH formation and the existence of primordial BHs [Jana et al., MNRAS Letters (2024)].
- *"Can we further the understanding or observation of the electromagnetically sourced nonlinearities in BH ringdown?"*

Current Section

Bardeen-Press-Teukolsky (BPT) equations

We consider a Schwarzschild BH with mass M that is perturbed by a sourceless electromagnetic field

$$\phi_2 = \varepsilon \phi_2^{(1)} + \mathcal{O}(\varepsilon^2). \tag{1}$$

Thus, the gravitational perturbation is nonlinearly sourced at the leading order

$$\Psi_4 = \varepsilon^2 \Psi_4^{(2)} + \mathcal{O}(\varepsilon^3). \tag{2}$$

The system of equations under consideration reads[1]

$$ {}_{-1}\mathcal{T} \phi_2^{(1)} = {}_{-1}\mathcal{S} = 0, \tag{3}$$

$$ {}_{-2}\mathcal{T} \Psi_4^{(2)} = {}_{-2}\mathcal{S}(\phi_2^{(1)}; \phi_2^{(1)}). \tag{4}$$

[1] For an explicit expression of the source term ${}_{-2}\mathcal{S}$, the audience is referred to our paper.

Coordinates and tetrad

To avoid complicated boundary condition problems and to extract astrophysically relevant results at future null infinity, we use horizon-penetrating hyperboloidally compactified coordinates $\{T, R, \theta, \varphi\}$, related to the Schwarzschild coordinates $\{t, r, \theta, \varphi\}$ via

$$\begin{aligned} T &= t - r + 2M \ln \frac{r - 2M}{2M} - 4M \ln \frac{r}{2M}, \\ R &= \frac{L^2}{r}, \end{aligned} \tag{5}$$

Future null infinity $\mathcal{I}^+$ is located at $R = 0$, and future event horizon $\mathcal{H}^+$ is located at $R_{\mathsf{H}} = L^2/2M$. Note that the hyperboloidal time coordinate T approaches a retarded time u when $R \to 0$ and approaches an advanced time v when $R \to R_{\mathsf{H}}$.

The hyperboloidal foliations in the Schwarzschild BH spacetime

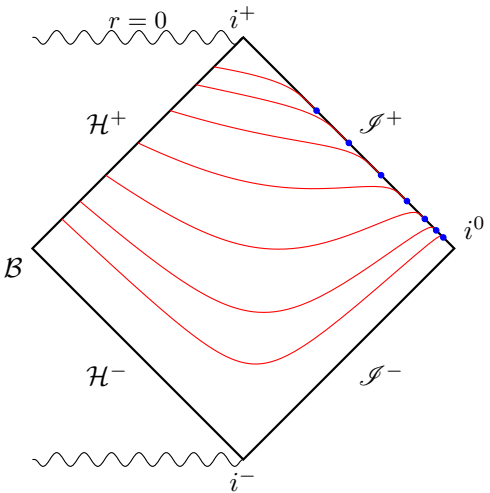

Coordinates and tetrad

A rotated Kinnersley tetrad, which is regular on the horizon, is used in this work

$$l^\mu = \frac{R^2}{L^4}\left\{4M^2, -\frac{1}{2}(L^2 - 2MR), 0, 0\right\}, \tag{6}$$

$$n^\mu = \left\{2 + \frac{4MR}{L^2}, \frac{R^2}{L^2}, 0, 0\right\}, \tag{7}$$

$$m^\mu = \frac{R}{\sqrt{2}L^2}\left\{0, 0, -1, -\frac{\mathrm{i}}{\sin\theta}\right\}. \tag{8}$$

Bardeen-Press-Teukolsky equations

In our coordinates and tetrad, the BPT equation reads

$$\left(C_{TT}\partial_T^2 + C_{TR}\partial_T\partial_R + C_{RR}\partial_R^2 + {}_sC_T\partial_T + {}_sC_R\partial_R + {}_sC - {}_s\not{\Delta}\right){}_s\hat{\psi} = {}_s\hat{\mathcal{S}}. \quad (9)$$

The relation between the rescaled scalars ${}_s\hat{\psi}, {}_s\hat{\mathcal{S}}$ and the NP scalars is

s	${}_s\hat{\psi}$	${}_s\hat{\mathcal{S}}$
-2	Ψ_4/R	$(2L^4/R^3)_{-2}\mathcal{S}$
-1	ϕ_2/R	$(2L^4/R^3)_{-1}\mathcal{S}$

We expand ${}_s\hat{\psi}$, as well as ${}_s\hat{\mathcal{S}}$, in terms of the spin-weight spherical harmonics ${}_sY_{lm}(\theta,\varphi)$,

$${}_s\hat{\psi}(T,R,\theta,\varphi) = \sum_{l,m} {}_s\hat{\psi}^{[lm]}(T,R){}_sY_{lm}(\theta,\varphi). \quad (10)$$

$${}_s\not{\Delta}{}_sY_{lm}(\theta,\varphi) = -(l-s)(l+s+1){}_sY_{lm}(\theta,\varphi) \quad (11)$$

Current Section

Analytical mesh refinement

Using only Chebyshev-Gauss-Lobatto collocation points $\{R_i^{\mathsf{Cheb}}\}$ is inefficient to get accurate tail behaviors.

Due to the differences between the decay rates at $\mathcal{I}^+$ and finite radii, growing gradients close to the future null infinity $\mathcal{I}^+$ occur in the late-time profile of the master function ${}_s\hat{\psi}^{[lm]}$.

To solve this problem, we use analytical mesh refinement

$$R(\sigma) = R_{\mathsf{H}} \frac{\sinh[\kappa(\sigma+1)/2]}{\sinh \kappa}, \tag{12}$$

and work in $\{R_i^{\mathsf{AnMR}}\} = \{R(\sigma_i^{\mathsf{Cheb}})\}$ at late times.

Analytical mesh refinement

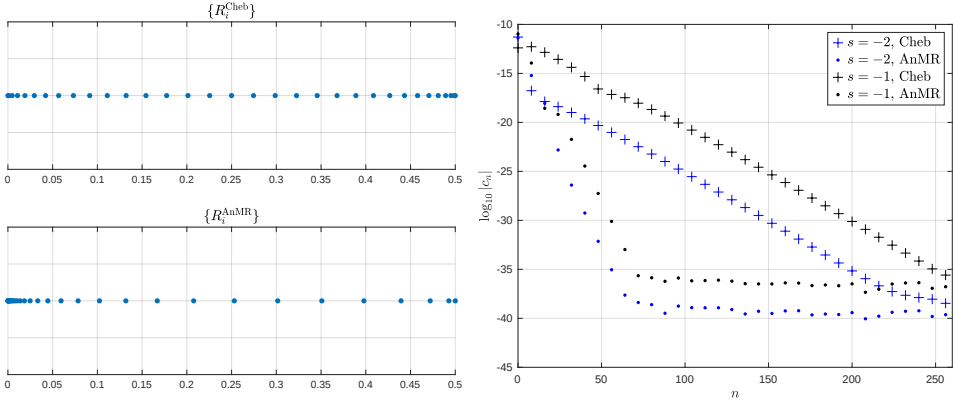

Figure 2: Left: With a mesh-refinement parameter $\kappa > 0$, $\{R_i^{\mathsf{AnMR}}\}$ are more dense near $R = 0$. Right: the spectral convergence of ${}_s\hat{\psi}$ at these two kind of points when a steep gradient occurs.

Time-symmetric integration

The time-symmetric integration method is ideal for long time numerical evolution in BH perturbation theory, which, compared with Runge-Kutta methods of the same order,

- is free of Courant limit,
- introduces smaller truncation error,
- and preserves Noether charges over long time periods.

We use a 4th-order time-symmetric integration method to solve an ordinary differential equation

$$\frac{\mathrm{d}\vec{u}}{\mathrm{d}T} = \vec{f}(T) \to \vec{u}_{n+1} = \vec{u}_n + \int_{T_n}^{T_{n+1}} \vec{f}\mathrm{d}T, \tag{13}$$

where the integrals are approximated by the Hermite rule

$$\int_{T_n}^{T_{n+1}} \vec{f}\mathrm{d}T = \frac{\delta T}{2}\left(\vec{f}_n + \vec{f}_{n+1}\right) + \frac{(\delta T)^2}{12}\left(\dot{\vec{f}}_n - \dot{\vec{f}}_{n+1}\right) + \mathcal{O}[(\delta T)^5]. \tag{14}$$

Current Section

Mode coupling

The mode coupling in the source term

$$ {}_{-2}\hat{\mathcal{S}}^{[l_3 m_3]} = \sum_{l_1 m_1} \sum_{l_2 m_2} {}_{-2}\hat{\mathcal{S}}({}_{-1}\hat{\psi}^{[l_1,m_1]}; {}_{-1}\hat{\psi}^{[l_2,m_2]}) \tag{15} $$

is determined by the corresponding Gaunt coefficients

$$ {}_{s_1}{}_{s_2}{}_{s_3}G^{m_1 m_2 m_3}_{\ell_1 \ell_2 \ell_3} = \int\int {}_{s_1}Y_{\ell_1 m_1} \cdot {}_{s_2}Y_{\ell_2 m_2} \cdot {}_{s_3}Y_{\ell_3 m_3} \sin\theta \, \mathrm{d}\theta \mathrm{d}\varphi \,. \tag{16} $$

We find that the power law of second-order tails does not depend on the mode coupling channels.

Results

A formal solution to the BPT equation can be obtained by the retarded Green's function $\mathcal{G}(T-T', R, R')$, i.e.,

$$ {}_s\hat{\psi}^{[l]}(T,R) = {}_s\hat{\psi}^{[l]}_{\mathsf{i}} + {}_s\hat{\psi}^{[l]}_{\mathsf{h}}, \tag{17} $$

where the inhomogeneous and homogeneous part read

$$ {}_s\hat{\psi}^{[l]}_{\mathsf{i}} = \int_0^T \int_0^{R_{\mathsf{H}}} \mathcal{G}\, {}_s\hat{\mathcal{S}}^{[l]}(T', R')\mathrm{d}R'\mathrm{d}T', \tag{18} $$

$$ {}_s\hat{\psi}^{[l]}_{\mathsf{h}} = \int_0^{R_{\mathsf{H}}} \left\{ {}_sP^{[l]}(T', R')\mathcal{G} - C_{TT}\, {}_s\hat{\psi}^{[l]}(T', R')\mathcal{G}_{,T'} \right\}_{T'=0} \mathrm{d}R', \tag{19} $$

respectively, with an auxiliary variable

$$ {}_sP^{[l]} = C_{TT}\partial_T\, {}_s\hat{\psi}^{[l]} + C_{TR}\partial_R\, {}_s\hat{\psi}^{[l]} + {}_sC_T\, {}_s\hat{\psi}^{[l]}. \tag{20} $$

The power law of second-order tails for $l \geq 4$

Our main result is that the late-time behavior of ${}_{-2}\hat{\psi}^{[l]}$, when $l \geq 4$, is dominated by the inhomogeneous part ${}_{-2}\hat{\psi}^{[l]}_{\mathrm{i}}$, suggesting a power law of the form

$$\begin{cases} T^{-2l-2} & \text{, at } \mathcal{H}^+ \text{ and finite radii} \\ T^{-l-3} & \text{, at } \mathcal{I}^+. \end{cases} \tag{21}$$

To see the dominant position of nonlinear tails over their linear counterparts more clearly, we solve both the inhomogeneous and homogeneous BPT equation under the same initial data (see Fig.3).

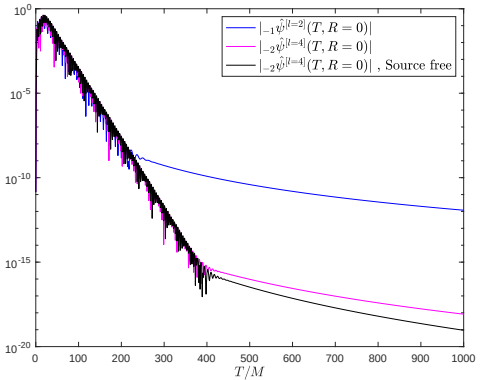

Figure 3: The waveform of ${}_{-2}\hat{\psi}^{[4]}$ and its parent ${}_{-1}\hat{\psi}^{[2]}$, as well as ${}_{-2}\hat{\psi}^{[4]}_{\mathrm{h}}$.

The power law of second-order tails for $l = 2$ and 3

However, when $l = 2$ and 3, the late-time behavior of ${}_{-2}\hat{\psi}^{[l]}$ depends on the competition between ${}_{-2}\hat{\psi}^{[l]}_{\mathsf{i}}$ and ${}_{-2}\hat{\psi}^{[l]}_{\mathsf{h}}$, determined by the initial data of ${}_{-1}\hat{\psi}$ and ${}_{-2}\hat{\psi}^{[l]}$ both. Interested in the effect of source term, we focus on results with the zero initial data for ${}_{-2}\hat{\psi}^{[l]}$ (${}_{-2}\hat{\psi}^{[l]}_{\mathsf{h}} = 0$).

- For ${}_{-1}\hat{\psi}$ with the compact support initial data, ${}_{-2}\hat{\psi}^{[l]}_{\mathsf{i}}$ decays as

$$\begin{cases} T^{-2l-3} & \text{, at } \mathcal{H}^+ \text{ and finite radii} \\ T^{-l-4} & \text{, at } \mathcal{I}^+. \end{cases} \tag{22}$$

- The non-compact support initial data of ${}_{-1}\hat{\psi}$, forming an extended source at the beginning, lead to a slower tail of ${}_{-2}\hat{\psi}^{[l]}_{\mathsf{i}}$ that conforms to the power law (21).

Comparison with recent analytical results

It was shown that the inhomogeneous part of Regge-Wheeler/Zerilli master function Ψ, induced by a compact outgoing source term $Q \sim 1/r^{\beta}$, decays as

$$\begin{cases} t^{-\beta-l} & \text{for } \beta = 0, 1, \\ t^{-2l-2} & \text{for } 2 \leq \beta \leq l+2, \\ t^{-2l-3} & \text{for } \beta \geq l+3, \end{cases} \tag{23}$$

at fixed spatial position [Ling et al., 2503.19967][2].
Our numerical result, i.e., the power law T^{-2l-2} at fixed spatial position when $l \geq 4$ for compact support ${}_{-1}\hat{\psi}(T=0,R)$, coincides with this analytical prediction (23) for the case $\beta = 6$.

[2]The same result for more general setup is empirically obtained by [Cardoso et al., 2405.12290].

Current Section

Implications for multi-messenger observations

- Despite still being strongly suppressed by the QNMs and neglected by any near-future observatories, the source-driven tails can be significantly amplified for binary BHs with high eccentricities, prospectively reaching the detection threshold of upcoming detectors.
- The electromagnetically sourced nonlinear tails differ from gravitationally sourced nonlinear tails when $l = 2, 3$, because the latter, with a source $Q \sim 1/r^2$, are dominated by the inhomogeneous part when $l \geq 2$, decaying as T^{-2l-2} at fixed spatial position.
- This difference, combined with the analysis of quadratic QNM, could help to identify astrophysical origins of GWs in the multi-messenger observations and offers a novel and complementary mechanism to detect black holes in the Milky Way.

Implications for multi-messenger observations

- It is the decay rate at null infinity $\mathcal{I}^+$ that is relevant for astronomical observations, due to extremely distant astronomical distances.
- The point closest to $\mathcal{I}^+$ in the numerical grid is located at $L^2/R^{\text{AnMR}}_{N'-1} \simeq 1.2 \times 10^6 M$, where the decay rate is almost the same as that at $\mathcal{I}^+$.
- the closest candidate for a supermassive black hole, Sgr A*, with a mass $M = 3.7 \times 10^6 M_\odot$ is about 26000 light years away, which roughly corresponds to $1.8 \times 10^9 M$ in the geometric units.

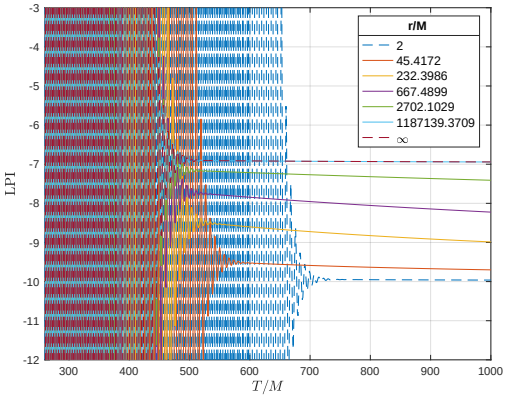

Figure 4: The distance-dependence of decay rates $p(T, R)$ for the second-order tails for $l = 4$.

Implications for multi-messenger observations

- We find that the peaks of GW waveform typically arrive at $\mathcal{I}^+$ later than those of their parent EM waveform in our simulations, indicating that EM events could be a forecast of their offspring GW events.
- The time difference $\Delta T \sim 10M$ of ${}_{-1}\hat{\psi}$'s peak and ${}_{-2}\hat{\psi}$'s peak roughly corresponds to 10^3 sec., if we set $M = 10^6 M_\odot$.

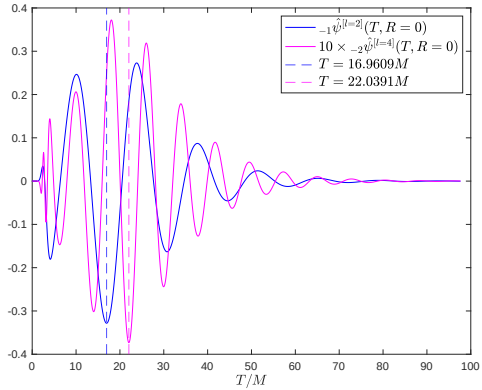

Figure 5: The waveform of ${}_{-2}\hat{\psi}$ and its parent ${}_{-1}\hat{\psi}$ extracted at $\mathcal{I}^+$.

Current Section

Summary

- Motivated by the desire to understand BH ringdown nonlinearities, we solve the inhomogeneous BPT equation numerically and find second-order gravitational tails induced by an electromagnetic source.
- Accurate numerical results are obtained by efficient numerical methods, including AnMR and time-symmetric integration.
- Our results suggest that the second-order tails of curvature perturbations with multipole numbers $l \geq 4$ decay as t^{-2l-2} at fixed spatial position and u^{-l-3} in retarded-time u at null infinity, slower than their linear counterparts.
- Our results can play a role in multi-messenger observations, e.g., identifying astrophysical origins of GWs and offering a novel mechanism to detect black holes in the Milky Way.

Thanks for your attention!